VIA MEDICA

ORIGINAL ARTICLE

Folia Morphol.
Vol. 79, No. 2, pp. 374–386
DOI: 10.5603/FM.a2019.0083

ISSN 0015–5659
journals.viamedica.pl

Comparative topographic analyses on the foramen magnums of two hystricomorphs: the crested porcupine (*Hystrix cristata*) and greater cane rat (*Thryonomys swinderianus*). Implications for typology, phylogeny and evolution in rodents

M.O. Samuel[1], N. Wanmi[1], J. Olopade[2]

[1]*Department of Veterinary Anatomy, Federal University of Agriculture Makurdi, Nigeria*
[2]*Department of Veterinary Anatomy, University of Ibadan, Nigeria*

[Received: 13 February 2019; Accepted: 1 April 2019]

Background: *This investigation aims to assess species comparison of foramen magnums in two hystricomorphs and endeavours an inter-species categorisation of individual shape outline.*

Materials and methods: *This study utilised 35 skull samples of different ages from the crested porcupine (H. cristata) (17) and the greater cane rat (T. swinderianus) (18) through. Elliptical Fourier Analysis, and the two-block Partial Least Squares analysis. Elliptical Fourier descriptor analyses presented marked amplitude related attenuations according to harmonics factor (1/10 to 2,980) in T. swinderianus though angular orientations in the major axis were not profoundly affected by size-normalisation in this species but up-regulated in H. cristata; (1/10 to1/95).*

Results: *Within and between groups analyses revealed PC1&2 contributed 98.94% and 1.06% but 100% PC1 between groups. The 1st to 4th harmonics gave full topographic description of the foramen magnums in both, 1st–3rd harmonics details compared differently revealing shape variance concentrated in posterolateral and posterior regions of the foramen magnum in the porcupine but antero-lateral and dorsal in cane rats, components of morphological asymmetry were demonstrated from 6th to 12th harmonics. Stepwise discriminant analysis of harmonic increments and Mahalanobis distance exposed increasing disparities between both up to the 5th harmonic (Bonferroni-corrected p-values [277.2, $p < 0.002$] group centroids) and a slightly lower value in variance for cane rats 0.421 and 0.378 for porcupines. A (58.3% and 33.3%); (94.1% and 11.1%) proportion before and after size-normalised evaluations of porcupines and cane rats size factor removal yielded 35.8% increase in accuracy among crested porcupines but 22.2% decline in cane rats. Dimorphic variations were less frequently expressed in cane rats corresponding to 33.3% and 44.2%. Size normalisation effect brought a reverse situation with an increased difference (11.1% in T. swinderianus; 5.9% in H. cristata). Individual specimen distribution along discriminant axis pooled by discriminant scores depicted less morphologic variability with greater overlaps.*

Address for correspondence: Dr. M.O. Samuel, Department of Veterinary Anatomy, Federal University of Agriculture Makurdi, Benue state, Nigeria, e-mail: walesamuel10@gmail.com

Conclusions: We observe that complexities in foramen magnum architecture between these indicates parcellation of shape and size variance and contributes as evidence for structural evolution, systematics, fundamental similarities and differences offers an explanation that both are related through evolutionary process of descent as baseline data and further support the suggestion; hystricidae in phylogenetic tree are better evolved and separate from thryonomidae. (Folia Morphol 2020; 79, 2: 374–386)

Key words: integration, modularity, foramen magnum, morphology, hystricomorpha

INTRODUCTION

The non-flat topography of the foramen magnum as a solid structure may be evaluated by model parametrisation through Elliptical Fourier Analysis (EFA) with regards to its peculiar scalar anisotropy and employed in discriminating among organism population.

Rodential species in Hystricomorpha group correctly comprises the Hystricidae (Porcupines), Bathyergidae (Sand-diggers), Thryonomydae (Grasscutters) and Petromuridae (African rock-rats) with the Phiomydis (African ancestry) as common tribe group. The crested African porcupine (*Hystrix cristata*) are more widely distributed in Sub-Saharan Africa, Italy and North America (Angelici et al. [3]) compared to a more geographically restricted Cane rats found exclusively in Africa with wide sub-regional distribution in West Africa [4, 35]. Represented by a single species, Thryonomys, most of the species, subspecies and breeds described may be aligned to one of the following groups: *T. swinderianus* (the larger/ /greater grasscutter) and *T. gregorianus* (the smaller grasscutter) [22].

Form and function have been shown to be present and correlated in shape change as adaptation to specific ecologies in a widespread range of organismal traits [24, 38]. The foramen magnum by its diverse morphology holds vital keys on skull topologic characterisation among species [17] but also presents peculiar challenges in its anatomic profiling [27]. Diversity in mammals is most represented in rodents, with astonishing ecomorphological diversification related to different locomotor types (cursorial, terrestrial, scansorial, arboreal and fossorial) and neurological functions [22, 28, 34]. From functional perspectives, studies on the foramen magnum can provide insights into the selective pattern operating during early ontogeny which ultimately determine the adult form of an organism [23]. This may help to understand systematic position in taxa, this structure is characterised by highly derived anatomical features more so that size and shape architecture presents important individual variations which demonstrate phylogenetic convergence in taxon [12]. The development of the foramen magnum depends largely on genetic composition, ecology and diet. Morphological variations in individuals, especially open and dorsal notches, have been linked to neuropathologic manifestations though without any certainty [27].

Importantly, different zygomasseteric conditions obtainable in rodents are not biomechanically equivalent and may enable rodents to be more efficient at different diet types. Hystricomorphy (possession of a large infraorbital foramen in Ctenohystrica + Anomaluromorpha + Dipodidae) through which the medial masseter passes as seen in Jerboas, porcupines and Capybaras [37] favouring efficient molar chewing whereas myomorphs are well adapted to all feeding modes and generates efficient incisor gnawing which may impact occipital area morphology [16].

Recent works has shown that these ecologically-driven shape changes, though mostly concentrated in the cranium, morphometric studies in this regard have played important roles in resolving taxonomic problems [9]. In comparison to studies in felids, it has been demonstrated that with skull and limbs measurements it was possible to correctly discriminate between species' Existing relevant works includes, Angelici et al. [3] who studied morphometric variations on the skull of the Italian crested porcupine (*Hystrix cristata*), Parés-Casanova [37] on *Hydrochoerus hydrochaeris*. More specifically our aim is to test the following hypotheses:

— Size influences subterranean shape differences between these species in ontogeny and allometric perspectives;
— Species follow distinct phenotypic patterns of skull components shape changes in relation to broad phylogenic distances;

Figure 1. Skulls of the crested porcupine (*H. cristata*) and greater cane (*T. swinderianus*) rat in caudal view showing the foramen magnum.

— There are no significant discriminations in subterranean shape and size for the foramen types in both species.

In this study we describe the morphology of the foramen magnums in two populations of hystricomorpha in order to characterise putative specialisations by comparing the anatomy of this structure in *H. cristata* to its closely related family member *T. swinderianus* relating it to morpho-physiology of locomotion and neurology in both species using the EFA descriptors in description of complex outlines as used by Urbanova [43] in which homology of landmarks are not important while details of shape outlines may be explained geometrically. The current investigation analyses of EFA descriptors of foramen magnum outlines employed variation-covariation by step-wise reconstructions in separate species groups irrespective of sex bias with contributions of principal components of the coefficients to assign quantities [26], compare both inter individual, interspecies variability and evaluate ontogeny. Here we test for shape and size covariations between the foramen magnums of the crested Porcupine and the Greater cane rat related to phylogenetic constraints.

MATERIALS AND METHODS

Skull acquisition and categorisation. For the purpose of this study 20 skull samples in equal composition and of different ages from the crested porcupine (*H. cristata*) and the greater cane rat (*T. swinderianus*) were obtained from around the same area (south-western region of Nigeria); a west African sub-region. Samples included for this investigation consist of complete skulls without apparent pathologies and were selected irrespective of sex. Some of these are from collections from the College of Veterinary Medicine, Federal University of Agriculture Makurdi, Benue State, Nigeria.

Foramen magnum outlines extraction. Using a digital camera (Canon® EOS equipped with EF-S 1200D, 18-55 IS 11 Kit, Hama tripod with plumb and stabilizer) in a direct focal plane, photographic images were taken in a direct caudal view of skulls without mandibles in place (Fig. 1) at a constant DIN of 25 cm to a central point on the foramen magnum. Transparent tracing paper with Cartesian co-ordinates was placed on captured images represented on the x, y co-ordinates. Based on Freeman encoding which allows us to represent edges in a numerical data structure which can be manipulated algebraically for extracting the elliptical Fourier descriptors (EFD). Images were processed in Microsoft paint as 24-bit depth BMP pictures at 2179 × 430 pixels specified for SHAPE chain coder (chain coder/Freeman edge encoding utilises a coding system in the description of geometrical information about contours/closed shapes numbered 0–7) programme software package for 2-D quantification and evaluation of biological shapes recognition and visualisation. It binarizes a full colour picture to black and white, in a clock-wise (y-x) direction the scanned outline tracings were digitally processed and data on foramen magnum outline contours were produced as Cartesian co-ordinates (x, y) on a scale of 50 mm [26, 43].

By using the geometric morphometric approach, variation in form can be captured and the allometric and non-allometric components can be disentangled [46].

To perform this analysis, we used EFA, and the two-block Partial Least Squares analysis [26, 29] developed for assessing covariation among divergent datasets (Fig. 2). Other analytical precautions were taken to ascertain the reliability of our results, including assessing the repeatability of the covariance matrices under resampling [33].

Elliptic Fourier sequences. In the classical elliptical Fourier approach [29] the previous parametric functions x(t) and y(t), describing the outline gives the expansion of the sequences as follows: (a*j*, b*j*) and (c*j*, d*j*) were the four Fourier coefficients defining each harmonic (j^{th} order); k corresponds to the maximum number of harmonics used for the Fourier decomposition and T was equal to the perimeter of the outline (see Fig. 2 above). The coefficients of elliptic Fourier descriptors can be mathematically normalised to be invariant to size, rotation and starting point of the contour trace. In SHAPE, the coefficients can be normalised by two types of procedures; one based on the ellipse of the first harmonic and the other based on the longest radius. For detailed information about the normalisation [29].

Size normalisation of foramen outlines coefficients. A recalculation of descriptors after size normalisation of foramen magnum outlines to be invariant of size was done based on first ellipse (first harmonic) using Chc 2-NEF SHAPE version 1.3 for obtaining the EFD descriptors values for the enclosed area in all samples evaluated [26]. Here four new descriptors were described for every harmonic in both species as follows:

— major axis length/2;
— minor axis length/2;
— orientation of the major axis;
— angle of phase corresponding to the position of the first point of the ellipse (θ = 1/2 arct.2 ($a_1b_1 + c_1d_1$)/$a_1^2 + c_1^2 - b_1^2 - c_1^2$).

Elliptical Fourier reconstructions. Stepwise reconstructions of foramen magnum outlines were carried out with incremental harmonics number employing descriptors derived from EFD.

Each harmonic ellipse was further evaluated by its size (major axis length/2 × minor axis length/2) as well as by anisotropy peculiar to each of them (major axis/minor axis) [6], where A_n, B_n, C_n and D_n are representing descriptors for the number of harmonics where n = number of harmonics.

$$x(t) = a_0 + \sum_{j=1}^{k} ajcos\left(\frac{2j\pi t}{T}\right) + \sum_{j=1}^{k} bjsin\left(\frac{2j\pi t}{T}\right)$$

and

$$y(t) = c_0 + \sum_{j=1}^{k} cjcos\left(\frac{2j\pi t}{T}\right) + \sum_{j=1}^{k} djsin\left(\frac{2j\pi t}{T}\right)$$

Figure 2. Elliptical Fourier sequences of co-ordinates descriptors of contours (x, y) as expanded by Dixon et al., 1997 [13] and permits description of an outline through series of harmonics; the geometry of each harmonic corresponds to an ellipse.

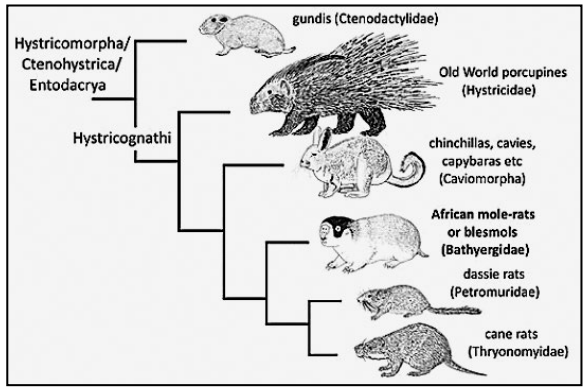

Figure 3. Phylogenetic hierarchy of the hystricomorpha, the old-world porcupines (Hystricidae) position relative to the cane rats (Thryonomidae) courtesy Darren Naish (http://blogs.scientific-american.com/tetrapod-zoology).

Visualising grid vectors displacement configurations, principal component and statistical analysis. Visual contributions of principal components of shape edge/outline coefficient descriptors analyses of foramen magnums of *H. cristata* and *T. swinderianus* was depicted with MorphoJ version 1.60 with grid-wire. Descriptors coefficients were analysed with 'PrinComp' based on Variance-Covariance matrix of normalised coefficients. It is also noted that such coefficients with small variance and covariation values do not significantly explain morphological variations and are now calculated and used in deriving the principal components bearing all information concerning edge/contour shapes in the first 12 harmonics [39]. Statistical analysis of this EFA data was done with paleontological statistics (PAST) version 3.0 [19] employing summary statistics (mean ± standard deviation [SD]) for descriptors. A species-based discriminant analysis with incremental harmonics in Fourier descriptors numbers, significance of the discriminant functions was assessed with Bonferroni post-test statistics and level of significance set at 0.05 and compared with the phylogenetic hierarchy (Fig. 3) diagram for confirmation.

Table 1. Species based *H. cristata* and *T. swinderianus* foramen magnum edge/contour in caudal view elliptical Fourier descriptors for the first 12 harmonics in summary (17 *H. cristata* and 18 *T. swinderianus*)

Harmonics	*H. cristata*			*T. swinderianus*		
	Major axis length/2 ± SD	Minor axis length/2 ± SD	Orientation of major axis (°)	Major axis length/2 ± SD	Minor axis length/2 ± SD	Orientation of major axis (°)
1	44.21 ± 0.81	4.07 ± 0.53	31.66 ± 0.09	45.43 ± 0.44	40.33 ± 0.58	17.93 ± 0.04
2	40.68 ± 0.66	40.11 ± 0.62	19.77 ± 0.24	48.11 ± 0.50	41.72 ± 0.44	14.81 ± 0.03
3	50.66 ± 0.73	48.09 ± 0.84	15.23 ± 0.15	51.55 ± 0.28	52.11 ± 0.39	24.07 ± 0.08
4	54.22 ± 0.89	43.00 ± 2.04	6.59 ± 0.17	50.91 ± 0.50	51.75 ± 0.35	216.48 ± 0.10
5	46.77 ± 1.68	35.24 ± 2.69	2.13 ± 0.38	51.51 ± 0.42	43.82 ± 3.04	47.18 ± 0.88
6	26.1 ± 2.98	17.02 ± 2.03	202.71 ± 0.79	47.32 ± 3.00	37.61 ± 3.46	40.14 ± 0.15
7	17.55 ± 0.58	15.31 ± 0.53	30.23 ± 0.06	25.81 ± 3.36	22.44 ± 2.63	39.50 ± 0.32
8	22.22 ± 2.19	21.22 ± 2.56	17.97 ± 0.11	15.35 ± 1.38	14.85 ± 1.38	121.84 ± 0.41
9	24.91 ± 2.73	20.37 ± 2.04	14.31 ± 0.69	13.61 ± 0.20	15.05 ± 0.44	86.51 ± 0.10
10	22.69 ± 0.34	22.51 ± 0.40	62.78 ± 0.05	15.72 ± 0.49	12.43 ± 0.22	45.68 ± 0.10
11	21.24 ± 0.37	20.44 ± 0.50	31.97 ± 0.03	17.97 ± 0.49	14.17 ± 0.44	45.23 ± 0.07
12	29.80 ± 0.93	28.51 ± 0.43	28.30 ± 0.05	28.12 ± 0.20	21.95 ± 0.69	45.23 ± 0.15

SD — standard deviation

Table 2. Species-based size-normalized *H. cristata* and *T. swinderianus* foramen magnum edge/contour in caudal view elliptical Fourier descriptors for the first 12 harmonics in summary (17 *H. cristata* and 18 *T. swinderianus*)

Harmonics	*H. cristata*			*T. swinderianus*		
	Major axis length/2 ± SD	Minor axis length/2 ± SD	Orientation of major axis (°)	Major axis length/2 ± SD	Minor axis length/2 ± SD	Orientation of major axis (°)
1	5.80 ± 0.16	4.31 ± 0.04	321.88 ± 640.50	4.72 ± 0.51	4.00 ± 0.43	5.23 ± 3.33
2	5.66 ± 0.06	4.83 ± 0.08	298.69 ± 622.67	0.21 ± 0.12	0.10 ± 0.03	61.37 ± 49.15
3	5.31 ± 0.01	4.82 ± 0.005	148.66 ± 411.72	0.30 ± 0.01	0.03 ± 0.01	209.86 ± 97.07
4	4.91 ± 0.02	4.72 ± 0.02	147.60 ± 280.68	0.04 ± 0.02	0.04 ± 0.03	88.10 ± 29.78
5	0.21 ± 0.01	0.11 ± 0.01	201.99 ± 642.15	0.01 ± 0.01	0.03 ± 0.01	51.51 ± 71.06
6	0.01 ± 0.01	0.03 ± 0.02	118.46 ± 162.82	0.004 ± 0.002	0.001 ± 0.01	44.97 ± 71.66
7	0.11 ± 0.01	0.01 ± 0.01	49.58 ± 49.81	0.003 ± 0.004	0.004 ± 0.005	217.26 ± 166.24
8	0.02 ± 0.005	0.01 ± 0.01	45.77 ± 177.82	0.02 ± 0.00	0.007 ± 0.003	271.23 ± 245.02
9	0.02 ± 0.004	0.01 ± 0.01	26.36 ± 65.95	0.004 ± 0.002	0.007 ± 0.002	110.42 ± 66.40
10	0.01 ± 0.01	0.03 ± 0.01	37.06 ± 59.46	0.007 ± 0.001	0.005 ± 0.002	26.20 ± 32.70
11	0.02 ± 0.005	0.00 ± 0.005	94.91 ± 39.07	0.004 ± 0.002	0.003 ± 0.001	89.63 ± 52.36
12	0.01 ± 0.005	0.01 ± 0.004	18.25 ± 28.24	0.005 ± 0.001	0.009 ± 0.001	51.61 ± 67.32

SD — standard deviation

Supplementary material for review

Validation of repeatability and measurement error. Measurements readings were taken as replicas at each run and recorded, a two-way Nonparametric multivariate analysis (NPMANOVA) at 9,999 permutations of both datum replica with Gower distances showed no significant values ($F = 1.933$, $P = 0.36$) therefore indicating high repeatability while an interclass correlation (0.96) indicated low influence of measurement error.

Compliance with ethical standards

The authors of this manuscript sought and obtained the permissions of the ethical committee of the College

Table 3. Species-based size-normalised *H. cristata* and *T. swinderianus* foramen magnum edge/contour in caudal view showing magnitude and anisotropy of the ellipses for the first 12 harmonics in summary (17 *H. cristata* and 18 *T. swinderianus*)

Harmonics	*H. cristata*		*T. swinderianus*	
	Elliptical magnitude ± SD	Elliptical anisotropy ± SD	Elliptical magnitude ± SD	Elliptical anisotropy ± SD
1	25.00 ± 0.88	1.35	18.88 ± 0.45	1.18
2	27.34 ± 0.12	1.17	0.021 ± 0.04	2.1
3	25.59 ± 0.07	1.10	0.009 ± 0.02	100.0
4	23.17 ± 0.05	1.04	0.002 ± 0.01	1.0
5	0.02 ± 0.04	1.91	0.0003 ± 0.01	0.3
6	0.0003 ± 0.02	0.33	0.000004 ± 0.01	4.0
7	0.001 ± 0.01	11.0	0.000012 ± 0.01	0.75
8	0.0002 ± 0.005	2.0	0.00014 ± 0.003	2.86
9	0.00008 ± 0.003	5.0	0.000028 ± 0.002	0.57
10	0.0003 ± 0.005	3.3	0.000035 ± 0.002	1.4
11	0.0002 ± 0.006	2.0	0.000012 ± 0.002	1.3
12	0.0001 ± 0.003	1.0	0.000045 ± 0.002	0.56

SD — standard deviation

of Veterinary Medicine, Federal University of Agriculture Makurdi, Benue State (CVM/FUAM/EC/022.2018)

RESULTS

Summary statistics and species-based quantitative analysis of EFD. Tables 1–3 shows the contributions of the first 12 harmonics of edge/contour for *H. cristata* (17) and *T. swinderianus* (18) and for size-normalised outlines, magnitude with the peculiar anisotropy of their ellipses. Fourier coefficients a_1, b_1 and c_1 d_1 are the constant normalised descriptors. Number of analysed harmonics for covariance is 14.

The series of increment in harmonics demonstrated a general gradual decline in major and minor axis lengths/2 in both species after an initial increase up to the 4th and 3rd harmonics irrespective of species and respectively (Tables 1, 2). Similar trends occurred in their elliptical magnitude values; in *H. cristata* this follows as earlier described decreasing through the first four harmonics, the 5th and 7th followed no particular order whereas *T. swinderianus* shows great disparity in this regard as it fluctuates in magnitude with values inferior to those in the crested porcupine (Table 3). From the 6th and 4th harmonics in *H. cristata* and *T. swinderianus* respectively these descriptors present values which are inferior or equal to 1% of the 1st harmonic values (Table 2).

The magnitudes of the ellipses assumed similar proportions earlier in the 5th and 2nd harmonics in both species respectively (Table 3).

Orientation of major axis corresponding to the third descriptor in both species (2.13–271) is not associated with any harmonic order but characteristic of both (Table 2).

In Table 3, the elliptical anisotropy (1.35–100) was characteristic of each harmonic in the species but did not represent any harmonic order.

Descriptor values revealed in size-normalisation results for the species showed marked amplitude related attenuations according to harmonics factor about (1/10 to 2,980) especially in *T. swinderianus* though angular orientations values of the elliptical major axis were not so affected by size-normalisation in this species but rather up-regulated in *H. cristata* according to harmonics (factor around 1/10 to1/95).

Topographic analyses of the stepwise reconstructions of the foramen magnum morphology in *H. cristata* and *T. swinderianus*

The 1st to 12th harmonics step-wise reconstructions of the foramen magnums of *H. cristata* and T. s*winderianus* shown in Figure 4 demonstrated better accuracy with increasing harmonic number as revealed in their fit indices shown visually by the representation (reconstructed vs. the original values) (Fig. 5). Out of 52 analysed principal component coefficients for both species comprised of 12 analysed harmonics in *H. cristata* and *T. swinderianus* and a total variance of 2.705687E-002 and 1.218013E-002, respectively (Supplementary Information, Table 4),

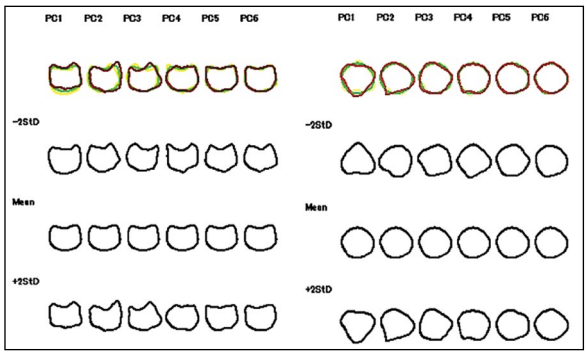

Figure 4. Foramen magnum outlines in *H. cristata* and *T. swinderianus* reconstructions for the first 18 harmonics (overlapped reconstructions = –2std = yellow, mean = green, +2std = red).

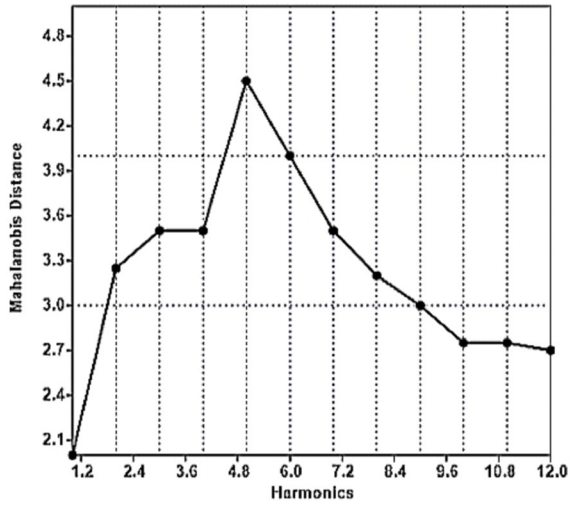

Figure 5. Fit diagram of *H. cristata* and *T. swinderianus* dissimilarity analysis of the foramen magnum outlines with harmonics increment calculated from discriminant analysis and Mahalanobis distance.

the first four principal components effectively elucidated the topography of the foramen magnums in the two species.

A within- and between-group analysis revealed PC1&2 contributed 98.94% and 1.06% of the variance within groups but 100% PC1 between groups (Fig. 6; *H. cristata* — green, *T. swinderianus* — red). By the 3rd and 4th harmonics in *H. cistata* and *T. swinderianus* respectively a full anatomical description was achieved on the foramen magnums of these species under investigation and finer details on the structure was clearly explained by the 12th. The inner outlines were the first to be defined by PC1 from a caudal view with the use of the 1st harmonic in reference to a central point in both type samples, the dorsal notch and right dorso-lateral condylar rims were topographically elucidated in crested porcupines but at variance in cane rat samples where the 1st harmonic explained left lateral condyle in clockwise direction by PC1. Taking a right ventro-lateral clockwise direction the 2nd harmonic described the left condylar rim and the ventral limits, whereas in cane rat samples it variably explained the right dorso-lateral condylar rims in *T. swinderianus* (Fig. 4, 7). The 3rd harmonics detailed its ventral limits of convergence and at variance with *H. cristata*'s left lateral rims. Components of morphological asymmetry was demonstrated from the 6th–12th harmonics between both species

Table 4. Eigen values and proportions in *H. cristata* and *T. swinderianus* species respectively showing coefficients whose percentage proportion values are greater than 1

Eigen value	Proportion (%)	Cumulative (%)	> 1/52
H. cristata			
PC1	1.071018E-002	39.5840	39.5840
PC2	6.919805E-003	25.5750	65.1590*
PC3	4.691780E-003	17.3404	82.4994*
PC4	2.179807E-003	8.0564	90.5558*
PC5	1.075084E-003	3.9734	94.5293*
PC6	6.385191E-004	2.3599	96.8892*
PC7	2.842671E-004	1.0506	97.9398
T. swinderianus			
PC1	4.998755E-003	41.0402	41.0402*
PC2	2.776223E-003	22.7930	63.8333*
PC3	1.721639E-003	14.1348	77.9681*
PC4	1.073403E-003	8.8127	86.7808*
PC5	4.629293E-004	3.8007	90.5815*
PC6	4.344384E-004	3.5668	94.1483*
PC7	2.150538E-004	1.7656	95.9139
PC8	1.459105E-004	1.1979	97.1118

*Significant Eigen values shown in by asterisk

Evaluation of species differences and polymorphism

A stepwise discriminant analysis of harmonics' increments and Mahalanobis distance revealed increasing disparities between the species up to the 5th harmonics (Fig. 5), after this harmonic further discrimination in evaluation became insignificant. The principal components contributions in the structure under investigation in both species shown in (Supplementary Information, Table 4, Fig. 7) as well as the first six reconstructions (Fig. 4) for *H. cristata* and *T. swinderianus*. An insignificant Mahalanobis

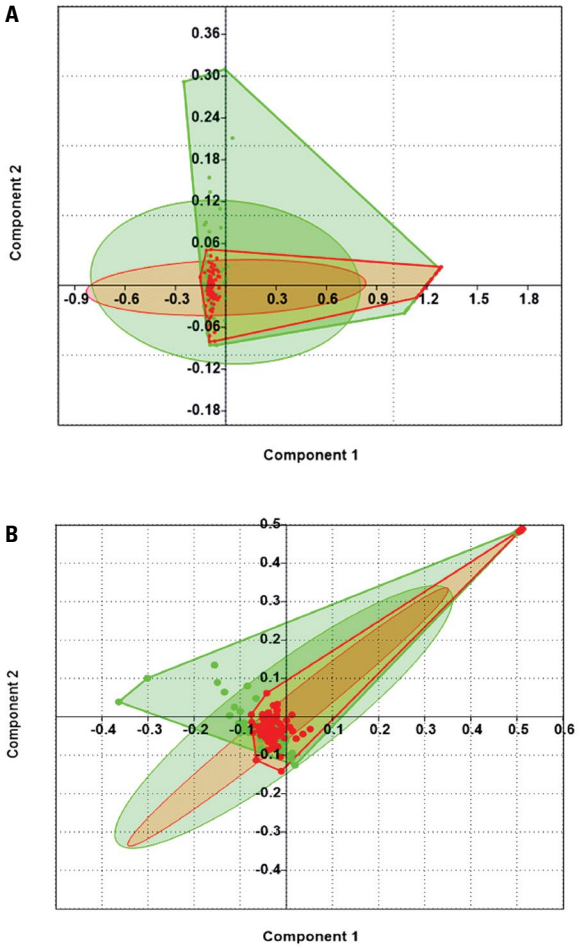

Figures 6. A, B. A comparative within- and between-group principal component analysis with convex hulls at 95% ellipses in *H. cristata* and *T. swinderianus* species foramen magnum; PC1&2 contributed 98.94% and 1.06% (within) and PC1 100% (between) respectively.

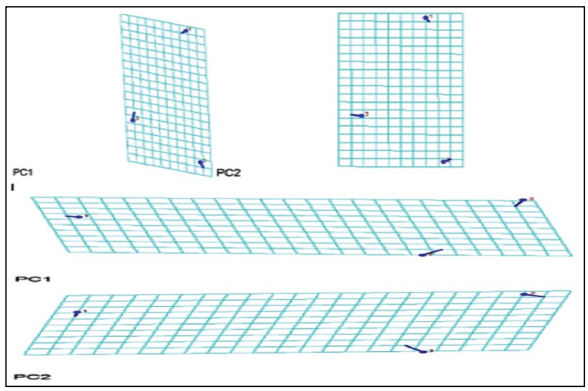

Figure 7. Grid wire visual representation of comparative principal components 1&2 contributions of foramen magnum contour outlines in *H. cristata* and *T. swinderianus* aligned by principal axis for the first 14 harmonics.

distance difference remained after size normalisation of foramen outlines (0.45, $p < 0.64$) after a discriminant elliptical Fourier descriptors evaluation as well as the Mahalanobis distance between species group centroids with Bonferroni-corrected p-values (277.2, $p < 0.002$). The cane rat demonstrated a slightly lower variance (0.421) in its variance co-variance matrix than the crested porcupines (0.378) 10th harmonics.

Table 5. Results of dimorphic classifications procedure of the size-normalised foramen magnum outlines performed from the elliptical Fourier descriptors (17 *H. cristata* and 18 *T. swinderianus*)

Species group	No. of individuals	Individuals classified as *H. cristata*	Individuals classified as *T. swinderianus*
H. cristata	17	10 (58.3%)	7 (41.2%)
T. swinderianus	18	6 (33.3%)	12 (66.7%)

Table 6. Results of dimorphic classifications procedure of the accurately classified foramen magnum outlines performed from the elliptical Fourier descriptors (17 *H. cristata* and 18 *T. swinderianus*)

Species group	No. of individuals	Individuals classified as *H. cristata*	Individuals classified as *T. swinderianus*
H. cristata	17	16 (94.1%)	1 (5.9%)
T. swinderianus	18	2 (11.1%)	16 (88.9%)

A 58.3% and 33.3% proportion of *H. cristata* and *T. swinderianus* individual samples respectively in the population presented significant polymorphism in the foramen magnum structural outline and it was 94.1% and 11.1% after size-normalised evaluation (Tables 5, 6). Size factor removal yielded a 35.8% increase in accuracy in crested porcupines but a 22.2% decline in greater cane rat. dimorphic variations in foramen magnum outlines was less frequently expressed by *T. swinderianus* than in *H. cristata*, this was found marginally significant and corresponded to 33.3% in *T. swinderianus*; 44.2% in *H. cristata*, size normalisation effect brought the reverse situation with an increased difference (11.1% in *T. swinderianus*; 5.9% in *H. cristata*).

Individual species specimen (y) distribution along the discriminant (x) axis when pooled according to discriminant scores depicted in (Fig. 8) for foramen magnum outlines and for size-normalised outlines, respectively. This diagram demonstrates vividly both the topographical anatomy and morphological variability possible between the crested porcupines and greater cane rats by such distribution. Species discrimination was less in size-normalised outlines but with greater overlap between them.

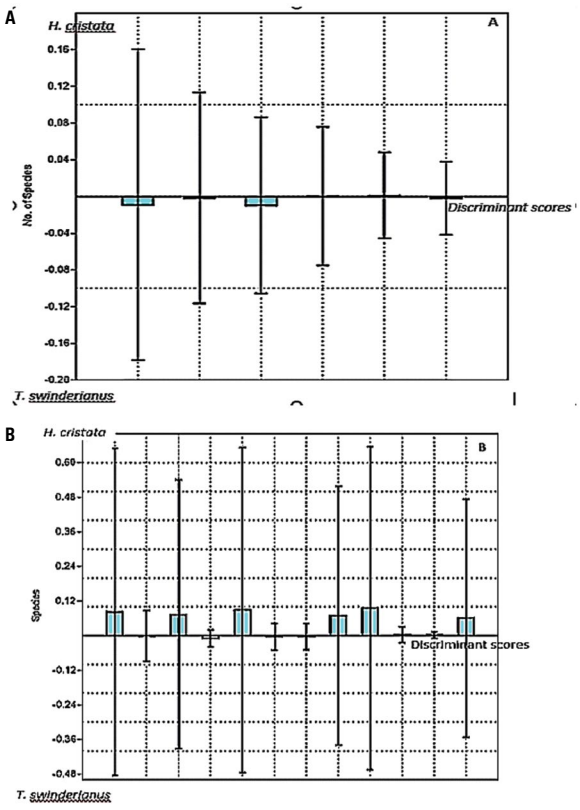

Figure 8. A, B. Analysis of polymorphism of the foramen magnum outline in caudal view. Showing distribution pattern of discriminant scores resulting from discriminant analysis of the elliptical Fourier descriptors with standard deviation and 95% interval in a centralised axis bar chat (B) for size-normalised foramen magnum outlines (17 *H. cristata* and 18 *T. swinderianus* specimens).

DISCUSSION

Choice of EFA methods for structural closed shape outline data decomposition. Rigorous shape analyses on solid structures is imperative when a necessity to distinguish species that differ in ecology, particularly regarding either prey size or locomotor style [31, 32] arise as in the current investigation to precisely topographically characterise the foramen magnum of two members of the same family in a caudal aspect with peculiar and often complex signatures to be biologically deciphered. EFA introduces scientific perspectives with ecological and anthropological interests in characterisation of foramen magnum outlines [42] and could be of forensic value. Polymorphism analysis, a phenomenon referred to as alternative phenotype and related to biodiversity, genetic and adaptation [1, 15] is further facilitated by this procedure.

The ease of connection with interpretations of geometry distinguishes the EFA from the classical Fourier coefficients [30] through its unique capacity to quantify closed shape outlines irrespective of its complexity, its step by step reconstruction permits easy evaluation of the four elliptical descriptors, its geometric details and morphologic inputs of every elliptical Fourier harmonics [30]; such inputs are then translated biologically to specific anatomic patterns. The 1st to 5th harmonics illustrate the general shape of foramen magnum outlines in both species whereas the later harmonics (6th to 12th) depict finer characteristic details of the structure (Fig. 4). It becomes possible to both quantify and clearly appreciate a convergence of result consequent to increase in harmonics as demonstrated by the fit index.

Reproducibility of the research methodology stems from relative ease of access to developed software packages for compatible personal computers facilitating image data processing from above 1,713 sample points on each specimen may suggest an enhanced accuracy, data compression and interpretation for analysis which can be moved from place to place and encourages quick dissemination for collaborating researchers.

Inter-specific discrimination in foramen magnum phylogenic and evolution. Recent studies have shown that cranial, dental and limb traits successfully separate species [31, 32], indicating both size and shape factors are vital traits peculiar to each rodent taxon from diverging ecologies [1]. Cranial topologic investigations among species are numerous in literature for evaluating skull typologies, taxa radiation and evolution [5, 44] as documented in molecular phylogenies and karyotypical evidence relating the Chaetomys skull closely to Erethizontidae rather than to the Echimyidae, despite occupying a relatively basal phylogenic position compared to the rest [44]. The high levels of molecular and morphological divergence suggested Chaetomys belongs to an early radiation of the Erethizontidae [44].

The rather inconspicuous location of the foramen magnum in the caudo-basal portion of skulls presents species-specific architectural challenges in quantitative and qualitative dimorphic and evolutionarily disparate or similar attributes [11]. Little or no comparative studies on this structure exist in literature for a between and within (hystricognathi) variabilities important for foramen magnum characterisation and categorisation in rodent systematics. Phenotypic characteristics in both species' foramen magnum showed inter-specific dissimilarities consistent with existing works [41, 42] and attributable to morphologic evolutionary interactions, these characteristics does not

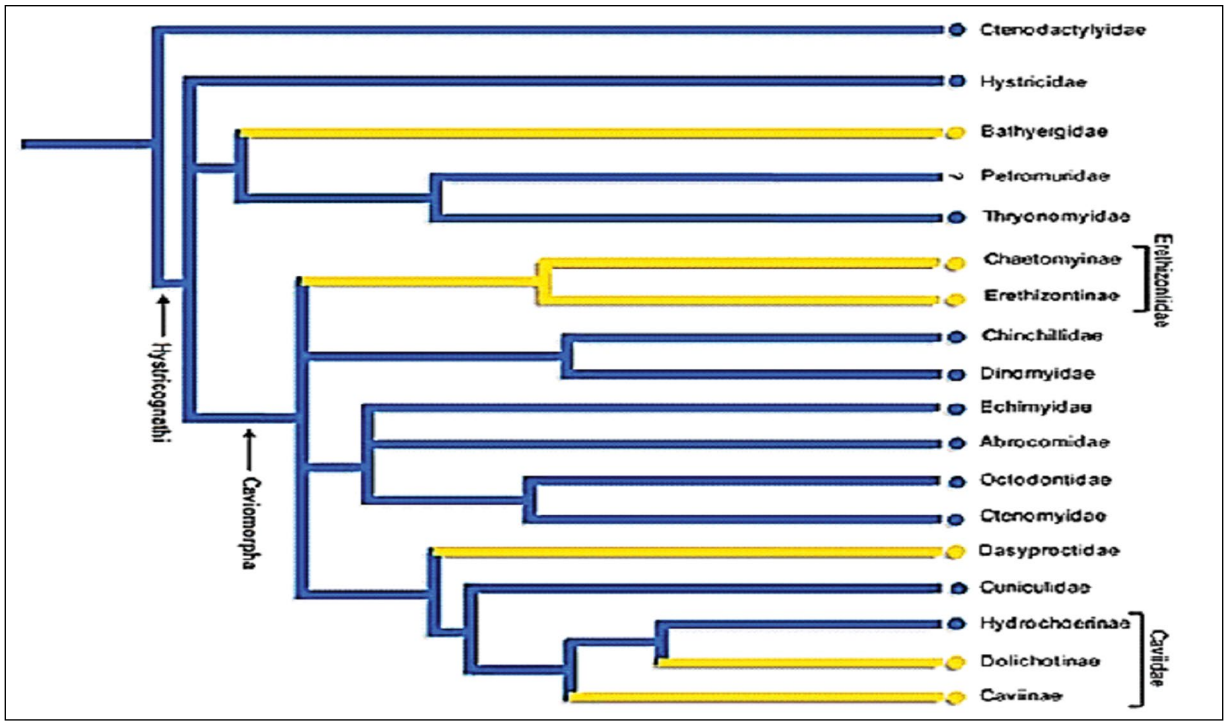

Figure 9. Phylogeny of the Hystricomorpha. Distribution of the single pair of interstitial-NOR-bearing chromosomes as a character in the phylogeny of Hystricomorpha based on published data herein presented courtesy (Mammalogy; Largomorpha, macroscelidea, RODENTIA-EEOB625, 2004). Blue branches indicate lineages with interstitial NORs. Yellow branches indicate lineages with terminal NORs. Blue circles indicate taxa with one pair bearing interstitial NORs. Yellow circles indicate taxa with one or more pairs bearing terminal NORs; NOR — nucleolar organising regions.

differentiate both on basis of bipedality or quadrupedality (locomotion) [10, 41] but may indeed predict foramen magnum angle reported to be dependent on auditory bulla size [16, 41]; this has not been prior reported in the current family under study. The crested porcupines presented a squarer outline and a relatively more robust construction with prominent condylar rims while the greater cane rats are more cylindrical, with dorsal and ventral notches and less elevated occlusive condyles [27]. A notable distinguishing qualitative feature of the foramen magnum is the dorsal and ventral notches in *H. cristata* and *T. swinderianus* respectively described and studied by DeLahunta [12] and Rusbridge and Knowler [40] in other species. The similar features observed in both structures is postulated to demonstrate phylogenetic affinity by their architectural convergence [8, 9] while the dissimilar may be attributed to integrative and modularity processes which are substrates in evolutionary processes in rodents [8].

Elliptical Fourier methods utilised in the current investigation permits a demonstration of significant monomorphic/dimorphic features in both species but at a higher proportion in *H. cristata* (41.2%, Table 5) *T. swinderianus* presented a slight reduction in this regard (33.3%) and could be attributed to usage of all information contained in the foramen magnum outline (1,713 retained sample points), the older metric method at best will yield incomplete morphological results. Non-discriminated proportion of samples observed could only be accounted for by further studies to determine sampling error, inadequate performance of applied method or a true inter-specific similarity of their foramen magnums and representative of biological trend.

Topographic components in comparative interspecific foramen magnum outlines morphology in Phylogeny. Size and shape are substrates to forms in foramen magnum outlines and precise individual signatures peculiar to species and those which are dimorphic represent a morphological challenge. Size factors are most useful in intraspecific sexual-size dimorphism while both size and shape elements give detailed topologic description of the considered structure [7, 11]. Figures 3 and 9 revealed a relative phylogenetic position of the species under study in the hystricognathi sub-family tree. It is admitted that higher species in the phylogeny tree of a group demonstrate better evolved body structures [20, 21]. Outside size-normalisation,

i.e. size and shape components of foramen magnum outlines, 58.3% and 66.7% are similar in the crested porcupines and cane rats outline, respectively, they are significantly dimorphic and dissimilar (41.2%, 33.3% in the same order) in both size and shape components in accordance with our second hypothesis. The organisation of the foramen magnum in the studied samples seem to be segregated along ecological and dietary lines since the greater cane rat must of necessity rotate the head forcefully to achieve complete severance and shredding of plant fibres. Asibey [4] suggesting a prominently developed foramen magnum lateral condyles though further studies in this direction may be necessary to confirm this observation. A constructed phylogenetic tree showing the most parsimonious trees by the branch and bound algorithm with a strict consensus of their average shapes by the Procrustes distance showed close similarity in clustering pattern and tree length (0) (Fig. 10).

Functional perspectives in comparative assessments of foramen magnum outlines during ontogeny between *H. cristata* and *T. swinderianus*. Ontogenetic changes in foramen magnum growth is associated with development in the presence of directionality from historical earlier to later time and from younger to older organisms [14, 45]. Evidence for its structural evolution explains the fundamental similarities between these species and have a straightforward explanation in the idea that both are related through an evolutionary process of descent from a common ancestor as observed in the house mouse (*Mus musculus*) [2], Marmots (*Sciuridae*) [8, 25], Salamanders (*Triturus spp.*) [22, 45] and the subfamily Caviomorpha [1]. As reported in other rodents the form of the posterior neurocranium might exert a constraint on the position of the brainstem, thereby increasing the chances of cerebellar protrusion indicated by volume reduction of the posterior fossa [41]. Furthermore, syringomyelia and neurological disorders remains potent with observations of open and dorsal notches occurrences frequently associated with captive breeding and domestication attempts [16], the concepts on which the fields of integration (i.e., the overall covariation of traits) and modularity (i.e., the relative autonomy of integrated structures, which are termed modules, from other structures) have been based [36]. Allometric variations with growth in *H. cristata* populations suggested 0.17% proportions (< 1%) demonstrated appreciable ontogenic similarity changes

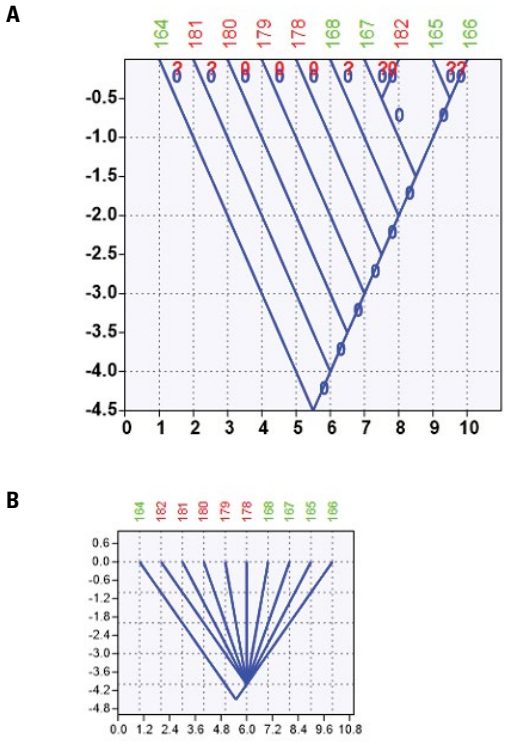

Figure 10. A, B. Parsimony analysis after samples to events (UA to RASC) using only FADS with Branch-and bound algorithm (Wagner optimisation) showing most parsimonious tree (MPT = 1) out of 2173623 evaluated, number of trees stored (10,000), tree length (0); **B.** Consensus tree.

whereas wide size variations (99%) occurred in this sampled population (Table 2). *T. swinderianus* had about 1.55% (≈ 2%) of its samples showing similarity in their sizes, hence wide functional differences exist with growth in both species demonstrating selective patterning with age variations [21, 22] differences. An inference of abnormal features' incidence as dorsal notches, condyle ventral limit arches can be made in the same proportions with reasonable accuracy (within sampling/methodology errors) [18].

CONCLUSIONS

We observe that the complexities demonstrated in foramen magnum architecture between these species investigated indicates parcellation of shape and size variance in the phylogeny and contributes as evidence of structural evolution in hystricignathii; where the crested porcupine occupies the topmost wrung of the phylogenetic ladder while the greater cane rat in the lowest wrung seems to be less evolved in comparison to the H. cristata in terms of foramen magnum structure. Foramen magnum size and shape development could be of value in hystricomorph systematics, also

fundamental similarities and dissimilarities offer offer an explanation which postulates that both species are related through evolutionary process of descent serving as baseline data and further supporting this suggestion that hystricidae in the phylogenetic tree are better evolved but separate from thryonomidae.

REFERENCES

1. Álvarez A, Perez S, Verzi D. Ecological and phylogenetic dimensions of cranial shape diversification in South American caviomorph rodents (Rodentia: Hystricomorpha). Biol J Linnean Society. 2013; 110(4): 898–913, doi: 10.1111/bij.12164.
2. Auffray JC, Alibert P, Latieule C, et al. Relative warp analysis of skull shape across the hybrid zone of the house mouse (Mus musculus) in Denmark. J Zool. 1996; 240(3): 441–455, doi: 10.1111/j.1469-7998.1996.tb05297.x.
3. Angelici FM, Capizzi D, Amori G, et al. Morphometric variation in the skulls of the crested porcupine Hystrix cristata from mainland Italy, Sicily, and Northern Africa. Mammalian Biol. 2003; 68(3): 165–173, doi: 10.1078/1616-5047-00078.
4. Asibey EOA. The grass cutter (Thyonomys swinderianus), TEMMINCK, in Ghana, Symp, Zool. Soc., London, 1974; 34: 161–170.
5. Bornert F, Choquet P, Gros C, et al. Subtle morphological changes in the mandible of tabby mice revealed by micro-ct imaging and elliptical fourier quantification. Frontiers Physiology. 2011; 2, doi: 10.3389/fphys.2011.00015.
6. Buck RC. Advanced calculus. 3rd ed. Waveland Press 1962: 252.
7. Calcagno J. On the applicability of sexing human skeletal material by discriminant function analysis. J Human Evolut. 1981; 10(2): 189–198, doi: 10.1016/s0047-2484(81)80017-6.
8. Cardini A. The geometry of the marmot (rodentia: sciuridae) mandible: phylogeny and patterns of morphological evolution. Syst Biol. 2003; 52(2): 186–205, doi: 10.1080/10635150390192807, indexed in Pubmed: 12746146.
9. Cardini A, Thorington RW. Postnatal ontogeny of marmot (rodentia, sciuridae) crania: allometric trajectories and species divergence. J Mammal. 2006; 87(2): 201–215, doi: 10.1644/05-mamm-a-242r1.1.
10. Charlesworth D. Evolution: A very short introduction. Oxford University Press, Oxford 2013: 10.1093/actrade/9780192802514.001.0001.
11. Cornette R, Herrel A, Cosson JF, et al. Rapid morpho-functional changes among insular populations of the greater white-toothed shrew. Biol J Linn Soc. 2012; 107(2): 322–331, doi: 10.1111/j.1095-8312.2012.01934.x.
12. DeLahunta R. Veterinary neuroanatomy and clinical neurology. 2nd ed. Saunders, Philadelphia, London 1983: 400–408.
13. Dixon AD, Hoyte DAN, Ronning O. Fundamentals of cranio-facial growth. Boca Raton, CRC Press, New York 1997: 155–185.
14. Drake AG, Klingenberg CP. The pace of morphological change: historical transformation of skull shape in St Bernard dogs. Proc Biol Sci. 2008; 275(1630): 71–76, doi: 10.1098/rspb.2007.1169, indexed in Pubmed: 17956847.
15. Drummond AJ, Rambaut A. BEAST: Bayesian evolutionary analysis by sampling trees. BMC Evol Biol. 2007; 7: 214, doi: 10.1186/1471-2148-7-214, indexed in Pubmed: 17996036.
16. Fabre PH, Herrel A, Fitriana Y, et al. Masticatory muscle architecture in a water-rat from Australasia (Murinae, Hydromys) and its implication for the evolution of carnivory in rodents. J Anat. 2017; 231(3): 380–397, doi: 10.1111/joa.12639, indexed in Pubmed: 28585258.
17. Fayolle P, Autefage A, Genevois P. La dysplacie occipital du chien. A propos d'une observation (in French). 1982; 133(1): 19–30.
18. Ginot S, Claude J, Hautier L. One skull to rule them all? Descriptive and comparative anatomy of the masticatory apparatus in five mouse species. J Morphol. 2018; 279(9): 1234–1255, doi: 10.1002/jmor.20845, indexed in Pubmed: 30117607.
19. Hammer Φ. Harper DAT. Ryan PD. Paleontological statistics software package for education and data analysis 2013; (Palaeontologicaz Electronica, 4; p9). http://palaeo-electronica.org/2001_1/past/issue1_01.htm (Assessed 14th February, 2012).
20. Hallgrímsson B, Willmore K, Hall BK. Canalization, developmental stability, and morphological integration in primate limbs. Am J Phys Anthropol. 2002; Suppl 35: 131–158, doi: 10.1002/ajpa.10182, indexed in Pubmed: 12653311.
21. Hallgrimsson B, Dorval C, Zelditch M, et al. Craniofacial variability and morphological integration in mice susceptible to cleft lip and palate. J Anat. 2004; 205(6): 501–517, doi: 10.1111/j.0021-8782.2004.00356.x.
22. Hautier L, Cox P, Lebrun R. Grades and clades among rodents: the promise of geometric morphometrics. Evolution of the Rodents: Advances in Phylogeny, Functional Morphology and Development (eds Cox PG, Hautier L). Cambridge: Cambridge University Press. 2015: 277–299, doi: 10.1017/cbo9781107360150.011.
23. Herrel A, De Smet A, Aguirre LF, et al. Morphological and mechanical determinants of bite force in bats: do muscles matter? J Exp Biol. 2008; 211(Pt 1): 86–91, doi: 10.1242/jeb.012211, indexed in Pubmed: 18083736.
24. Hutchinson JR. On the inference of function from structure using biomechanical modelling and simulation of extinct organisms. Biol Lett. 2012; 8(1): 115–118, doi: 10.1098/rsbl.2011.0399, indexed in Pubmed: 21666064.
25. Ivanović A, Vukov T, Džukić G, et al. Ontogeny of skull size and shape changes within a framework of biphasic lifestyle: a case study in six Triturus species (Amphibia, Salamandridae). Zoomorphology. 2007; 126(3): 173–183, doi: 10.1007/s00435-007-0037-1.
26. Iwata H, Ukai YA. SHAPE: A Computer Program Package for Quantitative Evaluation of Biological Shapes Based on Elliptic Fourier Descriptors. J Hered. 2002; 93(5): 384–385, doi: 10.1093/jhered/93.5.384.
27. Janeczek M, Chrószcz A, Czerski A. Morphological investigations of the occipital area in adult american staffordshire terriers. Anat Histol Embryol. 2011; 40(4): 278–282, doi: 10.1111/j.1439-0264.2011.01071.x.
28. Kay EH, Hoekstra HE. Rodents. Curr Biol. 1970; 18: 406–410.
29. Kuhl F, Giardina C. Elliptic Fourier features of a closed contour. Comput Graph Image Process. 1982; 18(3): 236–258, doi: 10.1016/0146-664x(82)90034-x.

30. Le Minor JM, Schmittbuhl M. Importance of elliptic Fourier methods for morphometry of complex outlines: application to the distal human femur. Surg Radiol Anat. 1999; 21(6): 387–391, doi: 10.1007/bf01631349, indexed in Pubmed: 10678732.
31. Meachen-Samuels J, Van Valkenburgh B. Craniodental indicators of prey size preference in the Felidae. Biol J Linnean Society. 2009; 96(4): 784–799, doi: 10.1111/j.1095-8312.2008.01169.x.
32. Meachen-Samuels J, Valkenburgh BV. Radiographs Reveal Exceptional Forelimb Strength in the Sabertooth Cat, Smilodon fatalis. PLoS ONE. 2010; 5(7): e11412, doi: 10.1371/journal.pone.0011412, indexed in Pubmed: 2062539.
33. Melo D, Garcia G, Hubbe A, et al. EvolQG - An R package for evolutionary quantitative genetics. F1000Res. 2015; 4: 925, doi: 10.12688/f1000research.7082.3, indexed in Pubmed: 27785352.
34. Musser GG, Carleton MD. Superfamily Muroidea. In: Mammal Species of the World: A Taxonomic and Geographic Reference, 3rd ed (eds Wilson DE, Reeder DM). Johns Hopkins University Press., Baltimore 2005: 122.
35. National Research Council (NRC). Micro livestock; Little Known Small Animals with a Promising Economic Future. National Academy Press, Washington DC, 1991: 449.
36. Olsen EC, Miller RL. Morphological Integration. University of Chicago Press, Chicago 1958: 23.
37. Parés-Casanova P. Mandibular allometry in Hydrochoerus hydrochaeris (Linnaeus, 1766) (Hydrocherinae, Caviidae). Papéis Avulsos de Zoologia (São Paulo). 2017; 57(35): 451, doi: 10.11606/0031-1049.2017.57.35.
38. Randau M, Goswami A. Shape Covariation (or the Lack Thereof) Between Vertebrae and Other Skeletal Traits in Felids: The Whole is Not Always Greater than the Sum of Parts. Evol Biol. 2018; 45(2): 196–210, doi: 10.1007/s11692-017-9443-6, indexed in Pubmed: 29755151.
39. Rohlf F, Archie J. A Comparison of Fourier Methods for the Description of Wing Shape in Mosquitoes (Diptera: Culicidae). Syst. Zool. 1984; 33(3): 302–317, doi: 10.2307/2413076.
40. Rusbridge C, Knowler SP. Coexistence of occipital dysplasia and occipital hypoplasia/syringomyelia in the cavalier King Charles spaniel. J Small Anim Pract. 2006; 47(10): 603–606, doi: 10.1111/j.1748-5827.2006.00048.x, indexed in Pubmed: 17004953.
41. Ruth AA, Raghanti MA, Meindl RS, et al. Locomotor pattern fails to predict foramen magnum angle in rodents, strepsirrhine primates, and marsupials. J Hum Evol. 2016; 94: 45–52, doi: 10.1016/j.jhevol.2016.01.003, indexed in Pubmed: 27178457.
42. Samuel OM, Casanova PM, Olopade JO. Elliptical Fourier descriptors of outline and morphological analysis in caudal view of foramen magnum of the tropical raccoon (Procyon cancrivorus) (Linnaeus, 1758). Morphologie. 2018; 102(336): 31–40, doi: 10.1016/j.morpho.2017.06.001, indexed in Pubmed: 29519615.
43. Urbanova P. VyuziTi meTod geOmeTricke mOFOmeTrie v BiOlOgii clOvekA A PriduzeNycH. OBOrecH masarykova univerzita Prirodovedecka faculta HABiliTAchni Prace, Brno 2010: 24–30.
44. Vilela RV, Machado T, Ventura K, et al. The taxonomic status of the endangered thin-spined porcupine, Chaetomys subspinosus (Olfers, 1818), based on molecular and karyologic data. BMC Evol Biol. 2009; 9: 29, doi: 10.1186/1471-2148-9-29, indexed in Pubmed: 19192302.
45. Weisensee KE, Jantz RL. Secular changes in craniofacial morphology of the Portuguese using geometric morphometrics. Am J Phys Anthropol. 2011; 145(4): 548–559, doi: 10.1002/ajpa.21531, indexed in Pubmed: 21541933.
46. Zelditch ML, Swiderski DL, Sheets DH. Geometric morphometrics for biologists: A Primer. 2.ed. . Elsevier Academic Press, San Diego 2012: 12.